Who Wins the Race Near the Interface?
– Stratification of Colloids, Nano-Surfactants and Others

Yifan Li[1], Matthew Marander[1], Rebecca Mort[1], Fei Liu[1], Xin Yong[2]*, Shan Jiang[1]*

[1]Department of Materials Science and Engineering, Iowa State University, Ames IA 50011
[2]Department of Mechanical Engineering, Binghamton University, Binghamton NY 13902

*Corresponding author, to whom all correspondence is addressed. Email: xyong@binghamton.edu; sjiang1@iastate.edu

Abstract

The diffusion of colloids, nanoparticles and small molecules near the gas-liquid interface presents interesting multiphase transport phenomena and unique opportunities for understanding interactions near the surface and interface. Stratification happens when different species preside over the interfaces in the final dried coating structure. Understanding the principles of stratification can lead to emerging technologies for materials fabrication and has the potential to unlock innovative industrial solutions, such as smart coatings and drug formulations for controlled release. However, stratification can be perplexing and unpredictable. It may involve a complicated interplay between particles and interfaces. The surface chemistry and solution conditions are critical in determining the race of particles near the interface. Current theory and simulation cannot fully explain the observations in some experiments, especially the newly developed stratification of nano-surfactants. Here we summarize the efforts in experimental work, theory, and simulation of stratification, with an emphasis on bridging the knowledge gap between our understanding of surface adsorption and bulk diffusion. We will also propose new mechanisms of stratification based on recent observations of nano-surfactant stratification. More importantly, the discussions here will lay the groundwork for future studies beyond stratification and nano-surfactants. The results will lead to the fundamental understanding of nanoparticle interactions and transport near interfaces, which can profoundly impact many other research fields, including nanocomposites, self-assembly, colloidal stability, and nanomedicine.

Introduction

Interfaces are crucial to numerous science and engineering fields, including nano-materials, phase transfer, and energy harvesting.[1-3] It has even been suggested that the presence of interfaces directly contributes to the origin of life. The ability to control the materials composition and properties at interfaces may lead to better medicines,[4] more efficient chemical reactions,[5] and next-generation energy storage devices.[6] Therefore, it is crucial to comprehend how molecules and particles move near the interfaces. In other words, who wins the race at the end? The answer will not only advance the fundamental knowledge of interface science, but also unlock transformative solutions to countless applications, including coating materials and drug formulations.

In general, the race near the interface can be determined through two steps. One is the diffusion through the bulk, which determines who gets to the finish line first;[7] the other is the adsorption to the surface,[8] which decides who can pass the finish line, stay at the surface, or replace other species at the interface. These two steps often interplay with each other and create a rather complicated scenario under different conditions. Therefore, many prior studies have created model systems that separate the two steps and only study them independently. For example, studies on stratification of colloidal mixtures through diffusion often chose particles that do not adsorb at the interface, while studies on surface adsorption often ignore the diffusion through the bulk.[9-12] In this perspective review, for simplicity, we will mainly discuss diffusion and adsorption separately, as the physics involved in each term is different. However, for many systems, it is critical to consider both to fully understand the phenomena observed in experiments and pave the way for engineering interfaces in practical applications.

An overview of different factors contributing to the final stratified structures and major physical processes has been summarized in **Fig. 1**. Early models of stratification simplified the system by eliminating the adsorption (using non-adsorbing particles) and ignoring interactions among particles (section 1, model 1). However, this model failed to explain many experimental observations. A more sophisticated model was developed by including the excluded volume of particles and diffusion of different particle species through structures formed by particles near the surface (model 2). Furthermore, a quantitative model was established by considering the interactions between colloids in the framework of colloidal diffusiophoresis (model 3). The system becomes even more complicated when incorporating charge and adsorption (sections 2 & 3). An epitomizing example is the stratification of nano-surfactants (section 4), which involves both diffusion and adsorption and presents a unique close-packed monolayer structure. When the particle size is small (< 50 nm), the adsorption becomes reversible, the scenario can be even more complicated.

One way to think about how different species race near the interface during a drying process is actually to consider their “escape” from the interface while the surface or interface is receding. Therefore,

diffusion plays a significant role in determining the final structure of a dried film consisting of a mixture of homogeneous particles. Diffusion rate quantifies the bulk particles' ability to move away from the surface, driven solely by thermal motion. Thus, different amounts of accumulation will occur at the drying front, depending on variances in the diffusion rate for various particle sizes. The scenario is described in the early theories by Routh and Russel *et al*.,[13] which introduced the Péclet number (Pe), *i.e*., the ratio of evaporation rate to diffusion rate, to predict stratification behavior. Under the same evaporation rate, a higher Pe number corresponds to slower diffusion, leading to particle accumulation near the receding interface during the drying process. However, this theory could not explain the experimental observations of fast diffusing small particles enriched at the top surface. To match experiments, Atmuri *et al*.[14] extended the diffusion model to include a surface interaction term illustrating how particle surface charge has an impact. Fortini *et al*.[15] presented a different model to explain particle migration in an osmotic pressure gradient, which is produced by the concentration gradient of particles towards the top of the drying film. This process was known as colloidal diffusiophoresis. The migration velocity of larger particles is qualitatively predicted to be higher in this model, leading to the small-on-top stratification. Zhou *et al*.,[10] Howard *et al*.,[16] and He *et al.*[17] further expanded on the quantitative theory of diffusiophoresis. Recently, the diffusiophoresis theory was extended to include hydrodynamic interactions and particle jamming, but these effects are still under lively debate.

As shown in **Fig. 2**, extensive work has been done on the investigation of small molecules,[18, 19] polymers,[20] colloidal particles,[21-23] and nanostructures[24] that are involved in stratification and transport near interfaces. However, very few previous experiments studied mixtures and the stratification of surface-active species. For example, surfactant molecules or particles with intermediate hydrophobicity, can adsorb strongly at surfaces and interfaces. When these are mixed with other species, the stratification behaviors can drastically change. Obviously, both adsorption and diffusion are important here. When the adsorption is reversible, the scenario can become even more complicated. One excellent example is the nano-surfactant, defined as amphiphilic nanoparticles with a Janus geometry.[25-27] When the concentration of Janus particles is high enough, aggregates and clusters may form, similarly to the micelles formed by the surfactant molecules. In addition, nano-surfactants are known to strongly adsorb at interface and form unique structures with surface active molecules.[28-30] The formation of these self-assembled structures will definitely change the fluid dynamics and stratification behaviors.

Recently, Li *et al.* studied the stratification behaviors of nano-surfactants.[31] It has been shown that when mixed with homogeneous particles, Nano-surfactants easily won the race to the interface and stratified into a complete and closely packed monolayer after solvent evaporation. Experimental data suggests that nano-surfactants move toward the interface three orders of magnitude faster than conventional Brownian motion, even across a significant distance (~ 200 μm) from the interface. The

intriguing question here is: why did nano-surfactants win the race to the interface so decidedly? Unfortunately, there is no clear explanation from current theory or simulation. Experimentally, conventional confocal microscopy is not responsive enough to accurately measure the fast dynamics. The experiments suggest that nano-surfactants are driven toward the interface by homogeneous particles, because the stratification only happens after mixing the two species. However, it is also noted that the system here is fundamentally different from "active particles" powered by external fields or surface reactions with fuels. In addition, the stratified structures of the mixtures are drastically different from clusters and fractal networks formed in the interfacial adsorption of pure Janus particles.[27, 28, 30, 32, 33] Furthermore, it is very unusual to observe particles stratified into a complete, close-packed monolayer, as all previously reported stratification only showed gradual concentration changes from the interface. Although the detailed mechanism for nano-surfactant stratification is unclear, we proposed a hypothesis based on the current experimental results later in this report.

Overview of stratification and its application

When a colloidal dispersion of particles with various sizes or surface chemistries is dried over a substrate, the colloids may self-separate into different domains or layers.[34-38] The direction of separation is normal to the surface or interface, having a regional variation in the local volume proportion of each type of particle. This phenomenon is called colloidal stratification. Facile and reproducible ways to control the colloidal stratification could enable innovations in many applications, including paints, inks, and adhesives.[39-42] For example, a stratified film can be used to form coatings with better performance. The lower region of the coating can be designed to have strong adhesion to the substrate, while the surface region can provide other functional properties, such as tackiness and water resistance.[43] In addition, compared with many surface engineering techniques, colloidal stratification is a much more effective way of tailoring surface properties of coating films from the bottom-up, which may significantly reduce the cost and usage of harmful solvents and additives. Understanding the mechanism of stratification will lead to novel formulations in the end applications. We will start with the discussion on theories of stratification of colloidal particles. Then we will consider adsorption and even broader systems including polymers and small molecules.

1. Diffusion and evaporation

Model-1: Competition between diffusion and evaporation rate

Single particle model and Péclet number

The simplest system to determine which important factors affect the particle distribution in the direction normal to the substrate is a monodisperse colloidal film. (**Fig. 3**).[44] The vertical drying of a dispersion

with evenly sized particles was modelled by Routh and Zimmerman.[45] The concentration of these particles near the film-air interface was higher when they were cast as a film.[13, 46] In the drying film, the evolution of particle distribution is governed by the competition between evaporation and diffusion. The characteristic timescale of particle diffusion is proportional to the square of the initial height of the film H and inversely related to the diffusion coefficient D: $\tau_{diffusion} \sim H^2/D$. The characteristic time for the film evaporation is proportional to H and inversely correlated with the rate of evaporation E (represented by the descending velocity of the surface): $\tau_{evaporation} \sim H/E$.[13] The Péclet number for the film formation is determined by the ratio of these two timescales:

$$Pe = \frac{\tau_{\text{diffusion}}}{\tau_{\text{evaporation}}} = \frac{\frac{H^2}{D}}{\frac{H}{E}} = \frac{6\pi\eta RHE}{kT}$$

Where η is the solvent viscosity, R is the particle radius, H is the initial film thickness, k is the Boltzmann constant and T is the temperature. Here, the Stokes-Einstein diffusion coefficient is $D = kT/6\pi\eta R$. The ultimate profile of dried films is determined by the Péclet numbers of the component particles. Based on the definition of a single-sized particle system, it is generally known that faster-diffusing small particles with Pe < 1 will be evenly distributed, and slower-diffusing large particles with Pe > 1 will accumulate at a descending air/water interface.[45]

Theory of stratification determined by Péclet number

Different scenarios are illustrated in **Fig. 4** and the relevant factors to be considered in those processes.[7] Diffusion and evaporation are the two most important factors. Routh and coworkers expanded on the single-particle model by taking into account a film with two different Péclet values and two particle sizes. Since the Péclet number is proportional to particle size when all the other conditions remain the same, a large particle always has a greater Péclet number. The first theory on stratification simply relies on the Péclet numbers. Within a drying particle suspension, the Péclet number of each component determines the dried film's final concentration profiles. For the colloidal mixture of two types of particles with different sizes, Peclet number for the large particles was defined as Pe_L, and for the small particles as Pe_S. In a binary mixture of large and small particles, if $Pe_L > 1$ and $Pe_S < 1$, bigger particles (which have higher Péclet numbers) are expected to accumulate more at the top surface due to the slower diffusion. In contrast, the fast-diffusing smaller particles with $Pe_S < 1$ will distribute more evenly across the film matrix. As a result, a self-stratifying matrix can be made.[47, 48]

However, Fortini *et al*. showed that stratification can be much more complicated.[15] In computer simulations of a binary mixture of spherical particles with diameter size ratio 7, they found the paradoxical "small-on-top" stratification in the regime of $Pe_L > Pe_S > 1$. An instance of colloidal

stratification in a drying process like this has never been reported. This striking result was subsequently corroborated by many other experimental and simulation studies. Interestingly, the Langevin dynamics simulation conducted by Tatsumi *et al*. further showed that, at a given particle size ratio, the evaporation rate does not affect this stratification monotonically.[49] There exists an optimal Péclet number at which the "small-on-top" stratification is mostly enhanced. Apparently, this behavior cannot be explained based only on the difference in the particle Péclet numbers because it would predict a "large-on-top" structure.

Model-2: Colloidal diffusiophoresis

A diffusiophoretic model was developed by Fortini *et al*. to resolve this counterintuitive "small-on-top" stratification, where both large and small particles have Péclet numbers greater than one.[15] The early Routh model does not consider the excluded volume of particles - in other words, the model allows particles to overlap with each other, which is unphysical. When excluded volume is considered, the accumulation of particles near the top of a drying colloidal film will create a concentration gradient induced by the descending interface when Pe > 1. Therefore, the particles diffusing through this layer will experience a corresponding osmotic pressure. Here, diffusiophoretic motion is referred to as the motion of colloidal particles in a concentration gradient created by other particles. In summary, the model describes three steps contributing to the observed "small-on-top" stratification: 1) arrest of both large and small particles with higher concentrations near the interface as a result of Pe > 1; 2) a downward osmotic pressure gradient is produced by the concentration gradient of particles near the top of a drying colloidal film; 3) larger particles have a stronger downward force than smaller ones.[50]

The Fortini model predicts that the segregation of individual particles can be determined by their relative downward velocity under the osmotic pressure gradient. The interaction between the large and small particles produces asymmetric effects on the phoretic drifts, which is a critical component of the diffusiophoretic model. Quantitatively, it was expected that in a binary mixture, the velocity difference of the large and small particles would scale with α^2 in the low-volume fraction regime and with α in the high-volume fraction regime. Here, α is the size asymmetry, defined as the size ratio of larger particles over smaller particles ($\alpha = d_L / d_S$). The size asymmetry also determines the difference in the Péclet numbers. Therefore, α is a critical parameter that controls the hierarchical structures of the matrix. Larger α tends to yield the "small-on-top" stratification. In short, the larger particles experience greater downward forces than smaller particles. Therefore, the larger ones are pushed farther away from the interfacial region by this diffusiophoretic force than their smaller counterparts.[16]

Furthermore, when φ_{small}, which is the volume fraction of the smaller particles near the interface, increases after specific level is reached (also depends on Pe_S), the larger particles are continuously pushed out of the interfacial zone by the diffusiophoretic force produced by the concentration gradient of the

small particles. As the interface continues to recede, the thickness of the layer depleted of large particles grows with time. As shown in **Fig. 5a**, Howard *et al*. investigated stratification in binary colloidal mixtures with implicit-solvent molecular dynamics simulations.[16] It is shown that with large particle size ratios and Péclet numbers greater than unity for all components, a stratified layer of small particles thickened and increased faster when α was higher, creating a "small on top" stratification.[51]

Statt *et al*. conducted non-equilibrium molecular dynamics simulations to compare the stratification behavior with and without explicit modeling of surrounding solvent, focusing on the influence of hydrodynamic interactions.[52] They modeled a binary mixture of long-chain and short-chain polymers as a surrogate system for colloidal mixtures. Their simulation results showed that the extent of stratification is overpredicted in previous numerical studies due to the absence of hydrodynamic effects from the solvent. The explicit solvent model highlights the necessity of incorporating hydrodynamic interactions into future modelling and simulations of stratification. However, including explicit solvents will demand a lot of computation power, which is challenging for many studies.

Since stratification is directly related to particle size, Martín-Fabiani *et al*. showed that stratification can be externally controlled by modulating the particle size with pH. The system contained pH-responsive smaller particles coated in hydrophilic poly(methacrylic acid) (PMAA) chains and large particles unaffected by pH. Under low pH, the PMAA chains became protonated, thereby reducing the charge and causing the chains to retract. When the pH was raised, these chains were deprotonated and extended as their affinity with water increased. Thus, the hydrodynamic diameter of small particles and the ratio between the large and small particles can be modulated by pH. As shown in **Fig. 5b**, at low pH (large α), they showed that an aqueous dispersion that was diluted and had an initial volume fraction of 0.1 stratified, with the smaller particles on top. When the pH was raised, small particles were swollen so that the size ratio decreased to 4.1 and the volume fraction increased up to 0.45. The stimuli-responsive change in the particle size results in the elimination of stratification. This strategy can be used to create smart coatings, which can be switched between homogeneous or stratified structures by controlling pH. These experimental results agree with the previous Langevin dynamics simulations on the effects of the particle size ratio.[9]

Model-3: ZJD model

Despite the success of the "colloidal diffusiophoresis" model in explaining the "small on top" stratification, a mechanistic understanding of diffusive driving force was missing in those early studies, leading to unsatisfactory predictions of stratification kinetics on the quantitative level.[51] To fill this gap, Zhou *et al*. provided a quantitative theory (commonly referred to as the ZJD model) in the framework of colloidal diffusiophoresis.[10] Similar to Trueman *et al.*,[34] they introduced an explicit expression of

chemical potential gradients of different-sized particles, which drive their diffusion. By assuming a dilute binary hard-sphere mixture, they approximated the free energy functional through the second-order virial expansion, from which the chemical potentials can be obtained. The second virial term captures colloid-colloid interaction, including the interactions between particles of the same size and those between particles of different sizes. The model reveals that the cross interaction between particles of different sizes has an asymmetrical impact on colloidal motion: it is much stronger on the larger colloids than on the smaller colloids and pushes the larger colloids towards the bottom of the film. Given the same magnitude of chemical potential gradients, the average velocity of the large particles is greater than that of the small particles. This difference in particle velocity results in the small-on-top structure. The ZJD model presents a critical improvement from the model proposed by Trueman *et al.*,[34] which did not consider the effect of inter-particle interactions. Zhou *et al.* also derived the condition required for stratification of small particles on top of large particles to be *"$\alpha^2(1 + Pe_S)\,\varphi_S > C$"*. In this equation, Pe_S is the Péclet number for the small particles, φ_S is the volume fraction of small particles and the constant C is taken to be on the order of one.[10] As shown in **Fig. 6**, Zhou *et al.* created the state diagrams to illustrate the parameter space where stratification is likely to occur. $\alpha^2(1 + Pe_S)$ is plotted versus φ_S in the ZJD diagrams, as shown in the red line. The region in the upper right corner, which lies above the boundary indicated by the equation, is expected to stratify small particles at the top. The region in the upper left corner, which lies above the boundary indicated by the equation, is expected to stratify large particles at the top. Figure 6 gives an example of a diagram with the size ratio was set as 7. Because the large particles' downward velocity is greater than the small particles', Zhou *et al*. discovered a number of variables where the large particles will remain concentrated at the top when close-packed.

Stratified structures created through the control of diffusion and evaporation

As the most feasible method to create stratified structures, tuning the drying conditions has been widely used for the experimental studies, Dong *et al.* showed stratification driven by the evaporation rate. Using aqueous mixtures of latex particles and ZnO nanoparticles at various evaporation rates, they developed and manufactured colloidal composite films (fast, medium, and slow). It was feasible to regulate the distribution of ZnO across the matrix of polymer nanocomposite films by tuning the evaporation rate and volume fraction of ZnO. The smaller ZnO nanoparticles migrated to the top surface of coating matrix during the drying process. As shown in **Fig. 7a-c**, the highest ZnO volume fraction and slow film drying were used to get the largest ZnO surface coverage.[53]

Despite the fact that trimodal and bimodal particle systems have been well explored, the case of polydisperse systems (multi-type particles exhibiting a broad distribution of sizes) has remained unexplored. Due to the widespread use of industrial powders and particles, such as inks, paints, and

coatings, are by nature polydisperse, it is essential to investigate the stratification involved in such systems. Cusola *et al*. suspended polydisperse colloidal particles in aqueous media and achieved polydisperse stratification via self-assembly induced by evaporation.[54] As shown in **Fig. 7d**, they found that the stratification of the particles which exhibit a wide range distribution of sizes could be adjusted by changing the drying conditions.

At intermediate drying rates, colloidal segregation in the various coating layers reached a maximum. As drying rates increased, the degree of segregation was reduced due to particle jamming. Using electron microscopy, cross-sectional imaging revealed a distinctive structure from that obtained by using particles with a mono or bimodal distribution. Polydisperse particles were segregated into different regions with various average sizes. Experimental findings and computer simulations suggested that the interaction of particle diffusion led to the development of segregation patterns. Utilizing similar strategies, Dong *et al*. synthesized an aqueous polydisperse colloidal system composed of smaller and larger zwitterionic particles, along with medium-sized standard acrylic binder particles.[55] Atomic force microscopy (AFM) showed that the content of both large and small zwitterionic particles in the film upper layer increased at faster evaporation rates, and the top surfaces could be covered mainly by zwitterionic groups for a variety of evaporation rates. Based on the differences in zeta potential, they hypothesized that a layer of large particles was trapped at the air/water interface and remained there after jamming. Thus large particles remained at the top of the dry film. Underneath, small particles were arranged above the medium particles, since the zeta potential of the medium particles was much greater than that of the small zwitterionic particles. They demonstrated that polydisperse systems are promising for overcoming the evaporation rate dependence of stratification processes in drying colloidal blends. This finding offers a route to enhance the robustness of stratification within coatings and other soft products where the evaporation rate cannot be finely tuned.

On the other hand, it is well known that increased drying temperature leads to increased evaporation rates and Péclet numbers. Evaporation-driven stratification has been studied under extreme conditions with the help of numerical simulations. Tang *et al*. explored ultrafast evaporation rates in their large-scale molecular dynamics simulations of binary colloidal film drying.[57] They simulated evaporation by allowing the solvent to escape into the vapor phase, leading to faster evaporation rates than those typical in physical experiments. Due to evaporative cooling induced by rapid evaporation, there were considerable temperature drops close to the film interface. A decreased density was found near the top interface as a result of the resultant temperature differential. They found that the particles moved under the density gradient by phoresis, and the effect was more substantial for the large particles. Thus, with ultrafast evaporation, large-on-top stratification was enhanced due to the phoresis in the cooling-induced

density gradient. This process overpowers the diffusive effects that lead to small-on-top stratification. They also showed that as the evaporation rate was decreased, the commonly seen "small-on-top" stratification was observed. Their findings underlined the significance of density gradients caused by rapid evaporation and demonstrated the necessity of properly describing the solvent when simulating evaporation-induced particle separation. Notably, the adsorption of colloidal particles at the interface can also drastically influence evaporation itself. Yong *et al*. performed many-body dissipative particle dynamics simulations to explore the evaporation of liquid film covered by nanoparticle monolayers.[58] They demonstrated that the adsorbed particles could suppress evaporation by reducing the accessible interfacial area and blocking the evaporation path of escaping vapor. These results suggest that stratification can be influenced by a complex interplay between evaporation, concentration change and particle adsorption. All these factors should be considered in future modelling and simulation of stratification.

Besides the stratification induced by the variance of diffusion and evoporation, which mostly manipulated by drying conditions, other synergistic approaches of controlling stratification for colloidal systems have been explored. Cardinal *et al*. reported an early example of stratification via combined mechanisms of Brownian diffusion, gravitational sedimentation, and evaporation.[59] As shown in **Fig. 8a**, the coating mixtures were composed of silica particles of two sizes. The dynamics of smaller silica particles were in the evaporation-dominant regime while the motions of large silica particles were dominated by sedimentation. Upon drying, the non-sedimenting small particles mainly accumulated into a thick layer at the top. **Fig. 8b** show that drying the suspension with poor colloidal stability leads to early sedimentation and inhomogeneous film.[60]

Although there have been comprehensive studies for colloidal stratification, both from simulations and experiments, there are notable limitations and gaps in the knowledge generated with these model systems. Therefore, it is challenging for the industry to develop product using the diffusive mechanisms. For instance, the Péclet number was hard to define and control in industrial fabrication. The volume fraction needed to be set accurately within an appropriate range to achieve reproducible stratification. Also, due to technical difficulties, only recent theoretical studies have started to consider the overcrowding/jamming effects, which are highly relevant in large-scale fabrication.

Commented [XY1]: Sedimentation is not relevant to diffusion and evaporation.

Commented [YL2R1]: Tried to briefly covered after the drying condition

2. Particle interactions and surface charge

The surface charge has been reported to induce self-stratification during film formation of latex blends. Previous simulations have shown that particle repulsions could repel particles away from the descending air interface in a drying film. Atmuri *et al*. simulated combinations of same sized particles, where one type was neutral and the other had charged repulsion.[14] They demonstrated a depletion region of repulsive

particles from the air interface. In the experiments by Nikiforow *et al*., blends of particles with similar sizes were studied.[62] Coatings with vertical concentration profiles in composition were fabricated by drying an aqueous colloidal dispersion containing both neutral and charged particles. Utilizing confocal microscopy, they observed that the neutral component was abundant at the air/film interface after drying. They concluded that the difference in collective diffusivity causes the two types of particles to separate vertically spontaneously. As the film dried, a layer enriched in both neutral and charge particles developed at the top. Because of to their mutual repulsion, charged spheres escaped from this layer more quickly than their neutral counterparts, assuming that the total drying time was appropriately chosen, between the diffusion times for the two types of particles. They comprehensively studied the experimental factors that cause segregation and demonstrate that collective dispersion, not preferential agglomeration or preferential wetting between the particles and the film/substrate interface, is what drives self-stratification in this context. Generally, charged particles strongly resisted accumulation at the film/air interface because of their mutual repulsion. They were driven away from the interface by electrostatic forces. Neutral particles also experienced repulsion, but this repulsion was short-ranged and only became important when the close packing of particles was almost reached. At that time, the dense packing prevented rearrangements of the particles, and the two species' concentration profiles in relation to one another were fixed.

Another important consideration involving particle interactions and the surface charge is colloidal stability. The balance between attractive and repulsive interactions between particles influences the colloidal stability in a suspension. An example of colloidal stratification via the colloidal stability was demonstrated by Grillet *et al*. Silica nanoparticles were mixed with polymer binders during the drying process.[60] The colloidal stability of the silica particles in the mixed suspension dictated the final morphology of the dry film. When water evaporation started for the stable mixed suspension, the silica particles distributed evenly throughout the entire matrix. When drying started for the suspension with poor stability, early aggregation took place and the silica clusters sedimented to the bottom. Thus, controlling aggregation enables the manipulation of the final morphology of the dry film. In the experiments of Sun *et al*., aqueous latex/ceramic nanoparticle dispersions were prepared. The pH was varied to control the colloidal stability, which further influenced the surface structures. Suspensions that formed less aggregates created coatings with higher percolation thresholds and higher transparencies than those made from unstable suspensions.[63]

3. Absorption

The effect of surface energy also plays a vital role in fabricating self-stratified coating systems. The phase with lower surface energy is driven to wet the air interface. There have been significant reviews and

literature on colloidal adsorption at the interface. Here we first focus on the contribution of adsorption during the drying and stratification process. Compared with other coexisting phases, polymers and latex with lower surface energy could be energetically favorable to form a thick wetting layer near the film-air interface during the drying process.[64] Generally, particle surface energy plays a role in the phenomenon of colloidal stratification in addition to the kinetic considerations. The work of Sun *et al*. and Roy *et al*. included the interfacial tension and thermodynamic considerations, making it energetically favorable for hydrophobic smaller particles to stratify to the interface that contains a layer of oil, so that the interfacial energy and surface tension of the system decreases.[65, 66] Most colloidal systems with low surface energy have been produced from fluorinated monomers. By seeded emulsion polymerization, Liu *et al*. synthesized a series of core-shell polyacrylate latexes with different silicone/fluorine monomer concentrations.[67] As shown in **Fig. 10**, the self-stratification properties of the core-shell latex films were verified by X-ray photoelectron spectroscopy and the static contact angle measurement. As the water dried, their results showed that the latex films displayed a preferential distribution of fluorinated composition near the matrix top surface. These core-shell fluorine/silicone-containing polyacrylate latexes are expected to be used within protective coatings with multiple functions, including anti-wetting, anti-icing, and corrosion-resistant properties.[68]

Exploring a similar idea, Wang *et al*. fabricated stratified semiconducting films with poly(3-hexylthiophene) (P3HT) and poly(methyl methacrylate).[69] The calculated surface energy of P3HT was lower than that of PMMA. This difference provided a strong driving force for P3HT to segregate at the air-film surface to minimize its surface energy. The vertically P3HT/PMMA are promising materials for organic thin-film transistors and are also suitable for fabrication on flexible substrates.

When the particle size is small enough, the adsorption becomes irreversible. Hua *et al*. demonstrated the competitive, reversible adsorption of nanoparticles and surfactants at fluid interfaces and independent control of both the adsorbed species accumulation with surface pressure.[11] **Fig. 11a,b** presents how both species they investigated interact reversibly with the interface. UV-vis adsorption and pendant drop measurements of the adsorption and surface pressure isotherms define the equation of state for the interface under conditions where the nanoparticles and surfactants are both in dynamic equilibrium with the bulk phase. They found that the free surface-active ions compete with nanoparticles for space at the interface and give rise to larger surface pressures upon the adsorption of nanoparticles. They also demonstrated reversible control of adsorbed nanoparticle amount through changes in the surfactant concentration or the aqueous phase pH. A recent study by Smits *et al*. brought about important understandings into how surface-active substances and nanoparticles interact and self-assemble at the liquid-liquid interface.[12] As shown in **Fig. 11c,d**, they investigated well-controlled model systems composed of hydrophilic, negatively, and positively charged silica nanoparticles and an oil-soluble

cationic lipid octadecyl amine (ODA) with in-situ synchrotron-based X-ray reflectometry, which is analyzed and discussed along with dynamic interfacial tensiometer. Their work indicated that negatively charged silica nanoparticles only adsorbed when the oil-water interface was covered with the positively charged lipid, suggesting synergistic adsorption. On the other hand, the positively charged nanoparticles readily adsorbed on their own but competed with octadecyl amine and reversibly desorbed with increased lipid concentrations. These results also suggest that through competitive adsorption, around the adsorbed particles there exists an electrostatic exclusion zone, thus preventing the adsorption of lipid molecules nearby and resulting in an unexpectedly high interfacial tension and a lower surface excess concentration of surfactants. These studies highlight the importance of adsorption and interfacial interaction of charged colloids and ionic surfactants for tuning the particle and surfactant contributions in complicated colloidal systems. Further studies should explore the competitive adsorption between nanoparticles and surface-active ions for the oil-water interface, through the reversible control of adsorbed amount via dynamic changes in the surfactant concentration or the aqueous phase pH. Potentially more sophisticated stratified structures can be achieved with fine control over the interface properties and surface packing densities.

4. Stratification of nano-surfactants

Nano-surfactants are created by integrating the features of both surfactants and nanoparticles.[70] Different from homogeneous nanoparticles, **nano-surfactants are defined as amphiphilic nanoparticles with a *Janus* geometry**.[26] As shown in **Fig. 12**, Li *et al*. recently reported nano-surfactants can self-stratify to a close-packed monolayer on top of a drying film when mixed with homogenous particles.[31] This unique feature enables the application of nano-surfactants as additives to improve the water resistance of conventional coating materials. Contrasting with homogeneous particle mixtures where stratification is driven passively by evaporation and form a concentration gradient near the surface, nano-surfactants can vigorously accumulate at the air-water interface with fast kinetics to form a complete and densely packed monolayer. The hydrophobic side faces the air, while the hydrophilic side maintains adhesion to the binder matrix, thereby forming a hydrophobic coating with strong adhesion. The weak adhesion issue of conventional hydrophobic coatings is addressed by this novel technology. Experimental work and preliminary theoretical model studies have shown that, unlike homogeneous particle mixtures that stratify largely through diffusion mechanisms, Janus particles have strong interfacial adsorption energy and can accumulate completely at the air-water interface with rapid kinetics, thus forming a self-stratified hydrophobic surface. It is well known that Janus particles can be thought of as colloidal surfactants that strongly adsorb at surfaces. The adsorption energy, defined as the interfacial energy change when a single particle moves from the bulk phase to the interface, is directly related to the Janus particle geometry. Janus particles with the perfect 50-50 (hydrophobic-hydrophilic) geometry have the highest

amphiphilicity, leading to the highest adsorption energy. The theoretical calculation also suggests that the more Janus geometry deviates from 50-50, the less adsorption energy is. The detailed mechanism is still under investigation; however, we propose that the self-stratification of Janus particles could be explained by the interplay in the following events (**Fig. 13**): (1) depletion of negatively charged binder particles from the interface due to the electrostatic repulsion; (2) accumulation of Janus particles toward the interface to balance the osmotic pressure which was generated from the binder particles; (3) Janus particles adsorbed irreversibly at the interface, due to their amphiphilicity and adsorption energy. They also showed that increasing the surface charge or the solvent's pH will strengthen the repulsion between the binder particles and the interface, therefore, increasing the osmotic pressure and expanding the depletion zone, and subsequently increasing the possibility for Janus particles to stratify onto the top surface. Developing Janus particles into highly efficient self-stratified coating additives offers cost-effective and commercially scalable solutions to many long-standing challenges in waterborne emulsion coatings, including water resistance, adhesion, surface hardness and film formation. With the unique monolayer and fast kinetics entailed by the chemical and structural properties of Janus particles, this finding also opens up new fronts for the study of Janus particles and offers a cutting-edge method for creating hierarchical structures that self-assemble. Beyond coating materials, this method may also find use in 3D printing, cosmetics, adhesives, and pharmaceutical formulations.

5. Perspective and Outlook of Colloidal Stratification

The study of the race near the interface will help us reveal the fundamental principles of colloid particle arrangement and diffusion near interfaces, which has far-reaching implications beyond stratification. The discovery will profoundly change our fundamental view of how interfaces alter the behaviors of colloids and nanoparticles. Although several models have already been established to explain the distribution of particle mixture of different species in a dried film, they are far from comprehensive. The interplay among particle interactions and surface adsorption has not been adequately addressed. The role of particle surface chemistry and the influence of added small molecules have not yet been fully explored. Experimentally it remains challenging to examine the behaviors of small nanoparticles.

On the other hand, the ability to modulate the surface properties through stratification will offer an innovative approach to addressing many long-standing challenges in the industry.[71, 72] For example, water-dispersible nano-surfactants can produce more durable water-resistant surfaces without the need for harmful organic solvents.[71, 73] Stratification can also be utilized to control the release of drugs and concentrate functional groups at the surface, such as anti-bacterial and anti-viral reagents, for producing innovative self-sanitizing coatings. These innovations may generate tremendous economic, health, and environmental benefits.

Acknowledgements

SJ would like to thank Iowa State University for the Start-up Fund and 3M for the Non-tenured Faculty Award. This work is partially supported by the State of Iowa Biosciences Initiative, American Chemical Society Petroleum Research Fund under Grants No. 60264-DNI7/56884-DNI9 and the Agriculture and Food Research Initiative Grant No. 2019-67013-29016 from the USDA National Institute of Food and Agriculture. This project/material also is based upon work supported by the Iowa Space Grant Consortium under NASA Award No. 80NSSC20M0107. XY would like to thank the National Science Foundation Grant No. 1939362 for partially supporting this work.

References

[1]K. Ariga, H. Ito, J. P. Hill and H. Tsukube, Chemical Society Reviews. **41**, 5800 (2012).
[2]S. Amemiya, X. Yang and T. L. Wazenegger, Journal of the American Chemical Society. **125**, 11832 (2003).
[3]M. Han, H. Wang, Y. Yang, C. Liang, W. Bai, Z. Yan, H. Li, Y. Xue, X. Wang, B. Akar, H. Zhao, H. Luan, J. Lim, I. Kandela, G. A. Ameer, Y. Zhang, Y. Huang and J. A. Rogers, Nature Electronics. **2**, 26 (2019).
[4]X. Zhang and D. G. Whitten, Langmuir. **27**, 1245 (2011).
[5]P. Davidovits, C. E. Kolb, L. R. Williams, J. T. Jayne and D. R. Worsnop, Chemical Reviews. **106**, 1323 (2006).
[6]X. Zhang, B.-W. Li, L. Dong, H. Liu, W. Chen, Y. Shen and C.-W. Nan, Advanced Materials Interfaces. **5**, 1800096 (2018).
[7]E. Gonzalez, M. Paulis, M. J. Barandiaran and J. L. Keddie, Langmuir. **29**, 2044 (2013).
[8]V. V. Verkholantsev, Pigment & Resin Technology. **32**, 300 (2003).
[9]I. Martín-Fabiani, A. Fortini, J. Lesage de la Haye, M. L. Koh, S. E. Taylor, E. Bourgeat-Lami, M. Lansalot, F. D'Agosto, R. P. Sear and J. L. Keddie, ACS Applied Materials & Interfaces. **8**, 34755 (2016).
[10]J. Zhou, Y. Jiang and M. Doi, Physical Review Letters. **118**, 108002 (2017).
[11]X. Hua, M. A. Bevan and J. Frechette, Langmuir. **34**, 4830 (2018).
[12]J. Smits, R. P. Giri, C. Shen, D. Mendonça, B. Murphy, P. Huber, K. Rezwan and M. Maas, Langmuir. **37**, 5659 (2021).
[13]A. F. Routh and W. B. Russel, Industrial & Engineering Chemistry Research. **40**, 4302 (2001).
[14]A. K. Atmuri, S. R. Bhatia and A. F. Routh, Langmuir. **28**, 2652 (2012).
[15]A. Fortini, I. Martín-Fabiani, J. L. De La Haye, P.-Y. Dugas, M. Lansalot, F. D'Agosto, E. Bourgeat-Lami, J. L. Keddie and R. P. Sear, Physical Review Letters. **116**, 118301 (2016).
[16]M. P. Howard, A. Nikoubashman and A. Z. Panagiotopoulos, Langmuir. **33**, 3685 (2017).
[17]B. He, I. Martin-Fabiani, R. Roth, G. I. Tóth and A. J. Archer, Langmuir. **37**, 1399 (2021).
[18]L. Huang, G. Wang, W. Zhou, B. Fu, X. Cheng, L. Zhang, Z. Yuan, S. Xiong, L. Zhang, Y. Xie, A. Zhang, Y. Zhang, W. Ma, W. Li, Y. Zhou, E. Reichmanis and Y. Chen, ACS Nano. **12**, 4440 (2018).
[19]H. Römermann and D. Johannsmann, The European Physical Journal E. **42**, 21 (2019).
[20]M. Schulz, R. W. Smith, R. P. Sear, R. Brinkhuis and J. L. Keddie, ACS Macro Letters. **9**, 1286 (2020).
[21]G. N. Sethumadhavan, A. Nikolov and D. Wasan, Langmuir. **17**, 2059 (2001).
[22]D. K. Makepeace, A. Fortini, A. Markov, P. Locatelli, C. Lindsay, S. Moorhouse, R. Lind, R. P. Sear and J. L. Keddie, Soft Matter. **13**, 6969 (2017).
[23]H. Luo, C. M. Cardinal, L. E. Scriven and L. F. Francis, Langmuir. **24**, 5552 (2008).
[24]P. Rocas, Y. Fernández, S. Schwartz, I. Abasolo, J. Rocas and F. Albericio, Journal of Materials Chemistry B. **3**, 7604 (2015).
[25]F. Liu, S. Goyal, M. Forrester, T. Ma, K. Miller, Y. Mansoorieh, J. Henjum, L. Zhou, E. Cochran and S. Jiang, Nano Letters. **19**, 1587 (2019).
[26]F. Liu, Y. Li, Y. Huang, A. Tsyrenova, K. Miller, L. Zhou, H. Qin and S. Jiang, Nano Letters. **20**, 8773 (2020).
[27]Y. Li, S. Chen, S. Demirci, S. Qin, Z. Xu, E. Olson, F. Liu, D. Palm, X. Yong and S. Jiang, Journal of Colloid and Interface Science. **543**, 34 (2019).
[28]K. Miller, A. Tsyrenova, S. M. Anthony, S. Qin, X. Yong and S. Jiang, Soft Matter. **14**, 6793 (2018).
[29]A. Tsyrenova, K. Miller, J. Yan, E. Olson, S. M. Anthony and S. Jiang, Langmuir. **35**, 6106 (2019).
[30]A. Tsyrenova, M. Q. Farooq, S. M. Anthony, K. Mollaeian, Y. Li, F. Liu, K. Miller, J. Ren, J. L. Anderson and S. Jiang, The Journal of Physical Chemistry Letters. **11**, 9834 (2020).
[31]Y. Li, F. Liu, S. Chen, A. Tsyrenova, K. Miller, E. Olson, R. Mort, D. Palm, C. Xiang, X. Yong and S. Jiang, Materials Horizons. **7**, 2047 (2020).

[32]T. G. Noguchi, Y. Iwashita and Y. Kimura, Langmuir. **33**, 1030 (2017).
[33]M. A. Fernandez-Rodriguez, M. A. Rodriguez-Valverde, M. A. Cabrerizo-Vilchez and R. Hidalgo-Alvarez, Advances in Colloid and Interface Science. **233**, 240 (2016).
[34]R. E. Trueman, E. Lago Domingues, S. N. Emmett, M. W. Murray and A. F. Routh, Journal of Colloid and Interface Science. **377**, 207 (2012).
[35]J. Wang, S. Ahl, Q. Li, M. Kreiter, T. Neumann, K. Burkert, W. Knoll and U. Jonas, Journal of Materials Chemistry. **18**, 981 (2008).
[36]D. Wang and H. Möhwald, Advanced Materials. **16**, 244 (2004).
[37]U. Steiner, J. Klein, E. Eiser, A. Budkowski and J. Fetters Lewis, Science. **258**, 1126 (1992).
[38]M. Geoghegan, R. A. L. Jones, R. S. Payne, P. Sakellariou, A. S. Clough and J. Penfold, Polymer. **35**, 2019 (1994).
[39]C. Gao, Y. Zhang, S. Mia, T. Xing and G. Chen, Colloids and Surfaces A: Physicochemical and Engineering Aspects. **609**, 125676 (2021).
[40]R. Jovanović and M. A. Dubé, Journal of Macromolecular Science, Part C. **44**, 1 (2004).
[41]E. Tekin, P. J. Smith and U. S. Schubert, Soft Matter. **4**, 703 (2008).
[42]S. A. Wissing and R. H. Müller, International Journal of Cosmetic Science. **23**, 233 (2001).
[43]J. Wang, X. Wang, C. Xu, M. Zhang and X. Shang, Polymer International. **60**, 816 (2011).
[44]M. Schulz and J. L. Keddie, Soft Matter. **14**, 6181 (2018).
[45]A. F. Routh and W. B. Zimmerman, Chemical Engineering Science. **59**, 2961 (2004).
[46]A. F. Routh and W. B. Russel, AIChE Journal. **44**, 2088 (1998).
[47]A. Gromer, M. Nassar, F. Thalmann, P. Hébraud and Y. Holl, Langmuir. **31**, 10983 (2015).
[48]A. Gromer, F. Thalmann, P. Hébraud and Y. Holl, Langmuir. **33**, 561 (2017).
[49]R. Tatsumi, T. Iwao, O. Koike, Y. Yamaguchi and Y. Tsuji, Applied Physics Letters. **112**, 053702 (2018).
[50]A. Fortini and R. P. Sear, Langmuir. **33**, 4796 (2017).
[51]M. P. Howard, A. Nikoubashman and A. Z. Panagiotopoulos, Langmuir. **33**, 11390 (2017).
[52]A. Statt, M. P. Howard and A. Z. Panagiotopoulos, The Journal of Chemical Physics. **149**, 024902 (2018).
[53]Y. Dong, M. Argaiz, B. He, R. Tomovska, T. Sun and I. Martín-Fabiani, ACS Applied Polymer Materials. **2**, 626 (2020).
[54]O. Cusola, S. Kivistö, S. Vierros, P. Batys, M. Ago, B. L. Tardy, L. G. Greca, M. B. Roncero, M. Sammalkorpi and O. J. Rojas, Langmuir. **34**, 5759 (2018).
[55]Y. Dong, N. Busatto, P. J. Roth and I. Martin-Fabiani, Soft Matter. **16**, 8453 (2020).
[56]W. Liu, A. J. Carr, K. G. Yager, A. F. Routh and S. R. Bhatia, Journal of Colloid and Interface Science. **538**, 209 (2019).
[57]Y. Tang, G. S. Grest and S. Cheng, Langmuir. **34**, 7161 (2018).
[58]X. Yong, S. Qin and T. J. Singler, Extreme Mechanics Letters. **7**, 90 (2016).
[59]C. M. Cardinal, Y. D. Jung, K. H. Ahn and L. F. Francis, AIChE Journal. **56**, 2769 (2010).
[60]A.-C. Grillet, S. Brunel, Y. Chevalier, S. Usoni, V. Ansanay-Alex and J. Allemand, Polymer International. **53**, 569 (2004).
[61]H. Römermann, A. Müller, K. Bomhardt, O. Höfft, M. Bellmann, W. Viöl and D. Johannsmann, Journal of Physics D: Applied Physics. **51**, 215205 (2018).
[62]I. Nikiforow, J. Adams, A. M. König, A. Langhoff, K. Pohl, A. Turshatov and D. Johannsmann, Langmuir. **26**, 13162 (2010).
[63]J. Sun, B. V. Velamakanni, W. W. Gerberich and L. F. Francis, Journal of Colloid and Interface Science. **280**, 387 (2004).
[64]A. Misra and M. W. Urban, Macromolecular Rapid Communications. **31**, 119 (2010).
[65]Y. Sun, Y. Zheng, C. Liu, Y. Zhang, S. Wen, L. Song and M. Zhao, RSC Advances. **12**, 15296 (2022).
[66]P. K. Roy, B. P. Binks, E. Bormashenko, I. Legchenkova, S. Fujii and S. Shoval, Journal of Colloid and Interface Science. **575**, 35 (2020).

[67]Z. Liu, Y. Zhao, J. Zhou and X. Yuan, Colloid and Polymer Science. **290**, 203 (2012).
[68]Y. Kim, H. J. Kwon, J.-W. Kook, J. J. Park, C. Lee, W.-G. Koh, K.-S. Hwang and J.-Y. Lee, Progress in Organic Coatings. **163**, 106606 (2022).
[69]X. Wang, W. H. Lee, G. Zhang, X. Wang, B. Kang, H. Lu, L. Qiu and K. Cho, Journal of Materials Chemistry C. **1**, 3989 (2013).
[70]S. Jiang, Q. Chen, M. Tripathy, E. Luijten, K. S. Schweizer and S. Granick, Advanced Materials. **22**, 1060 (2010).
[71]S. Jiang, A. Van Dyk, A. Maurice, J. Bohling, D. Fasano and S. Brownell, Chemical Society Reviews. **46**, 3792 (2017).
[72]M. Zubielewicz and A. Królikowska, Progress in Organic Coatings. **66**, 129 (2009).
[73]Y. Li, F. Liu, S. Chen, A. Tsyrenova, K. Miller, E. Olson, R. Mort, D. Palm, C. Xiang, X. Yong and S. Jiang, Materials Horizons. 2047 (2020).

Figures:

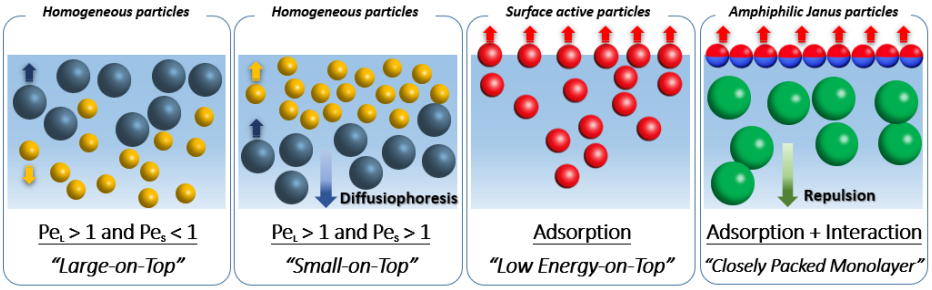

Fig. 1. Schematic illustration of four representative colloidal stratification processes with their corresponding structural features and driven factors. For the colloidal mixture of two types of particles with different sizes, Peclet number for the large particles was defined as Pe_L, and for the small particles as Pe_S.

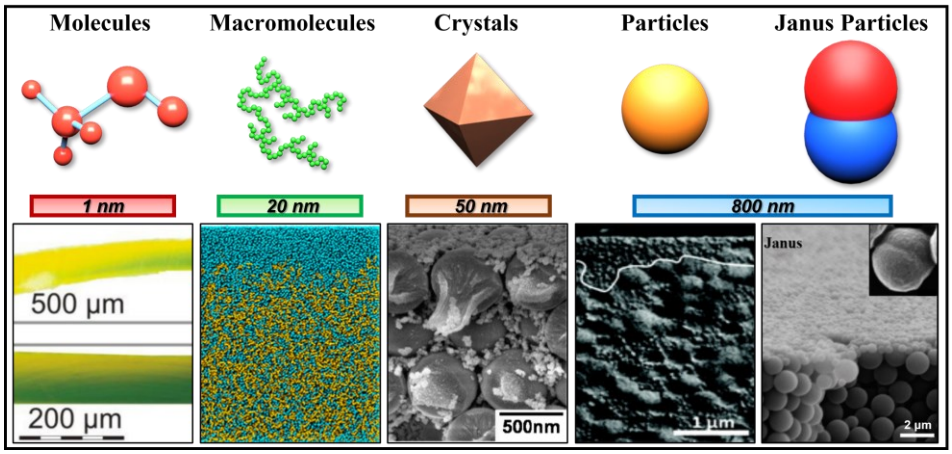

FIG. 2. Schematic chart of various items involved in stratification and transport near interfaces. Small Molecules, reproduced from ref. 19 with permission from the Springer Nature. Macromolecules, reproduced from ref. 51 with permission from the American Chemical Society, Crystals, reproduced from ref. 23 with permission from the American Chemical Society. Particles, reproduced from ref. 22 with permission from the Royal Society of Chemistry. Janus Particle structures, reproduced from ref. 31 with permission from the Royal Society of Chemistry.

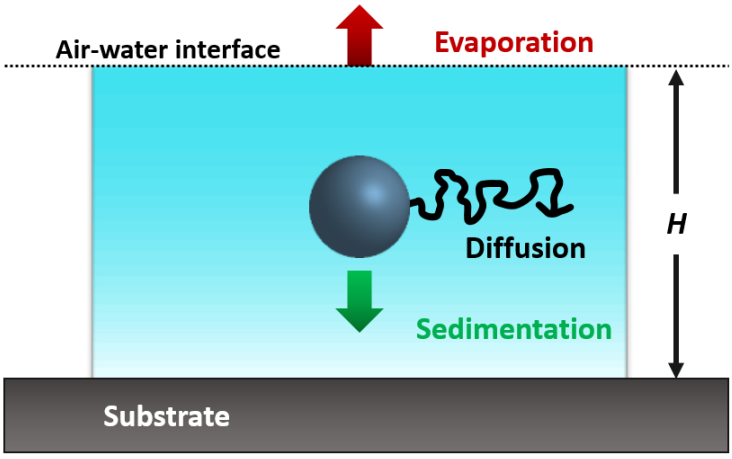

FIG. 3. Schematic diagram of factors that affect the distribution of particles in a colloidal film. A particle is suspended in a viscous liquid in a film of initial thickness, H. As a result of the evaporation of the continuous liquid phase, the top interface descends at a constant velocity. If the density of the particle is greater than the density of the liquid, then the particle will be subject to sedimentation. The particle will also undergo Brownian diffusion. Reproduced from ref. 44 with permission from the Royal Society of Chemistry.

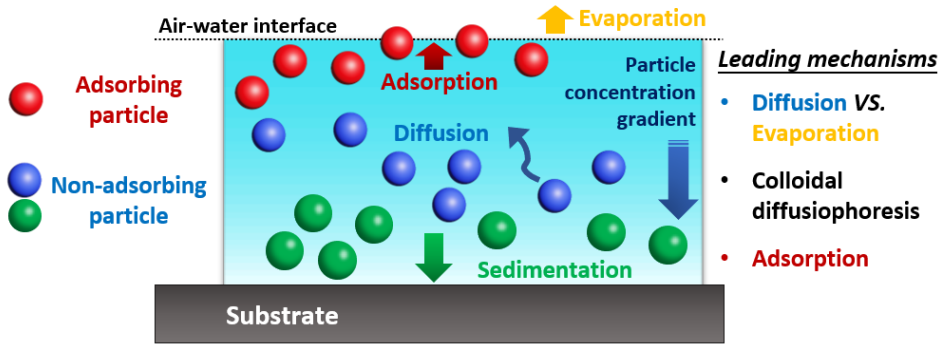

FIG. 4. Schematic diagram of factors that affect the distribution of particles in a colloidal film. As a result of the evaporation of the continuous liquid phase, the top interface descends, which will create a concentration gradient for particles. Different types of particles can be suspended in a viscous liquid. Studies have involved both adsorbing and non-adsorbing particles. Several mechanisms are proposed to explain the distribution of particles in the dried films. If the density of the particle is greater than the density of the liquid, the particles will also be subject to sedimentation. In addition, the particles exhibit Brownian diffusion.

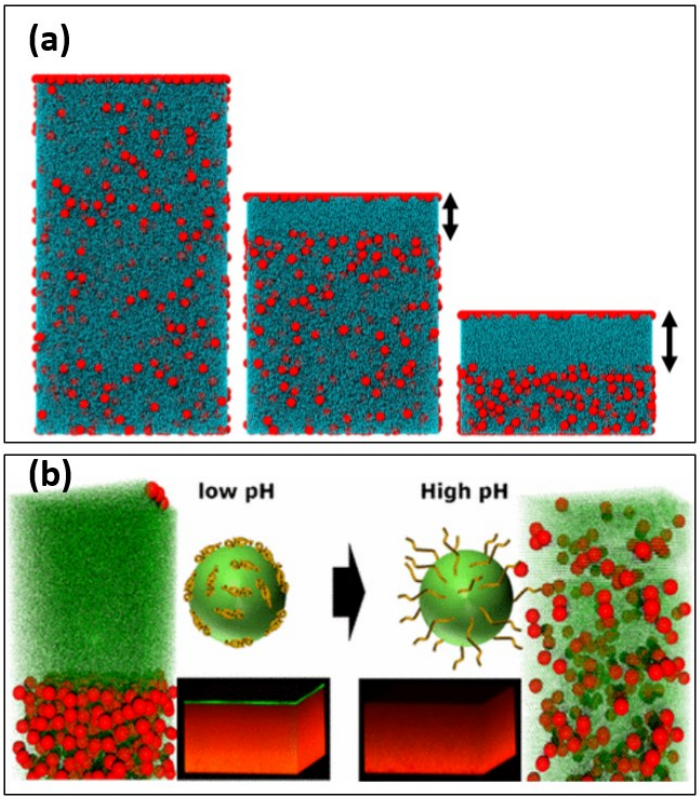

FIG. 5. (a) Snapshots of drying film at different time points. Arrows indicate the stratified layer of small colloids. Snapshots was captured using Visual Molecular Dynamics. Reproduced from ref. 16 with permission from the American Chemical Society. (b) On the left side, confocal image of a binary colloidal film with size ratios as 7.1 and initial total volume fraction of 0.1. The small particles contain a green fluorescent dye and are seen in a layer at the top of the film. A snapshot of the final structure obtained from Langevin dynamics simulations for this system is shown to the left. On the right side, image of the same materials system when size ratios as 4.1 and the initial volume fraction is 0.45. The red and green particles are distributed uniformly with depth. A snapshot of the corresponding Langevin dynamics simulations is shown to the right. Reproduced from ref. 9 with permission from the American Chemical Society.

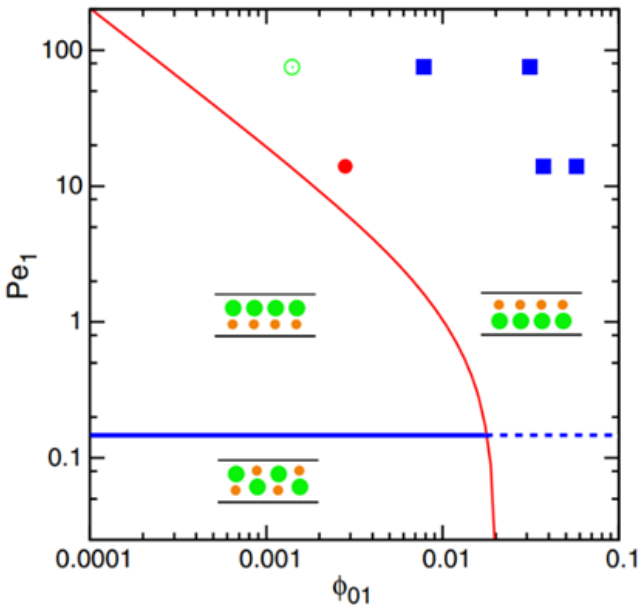

FIG. 6. When "α" was set as 7, a representative state diagram was derived from the ZJD model. The labels indicate the areas where stratification with large or small particles on top and homogeneously distributed particles are anticipated. The ZJD equation was used to calculate the red line. Reproduced from ref. 10 with permission from the American Physical Society.

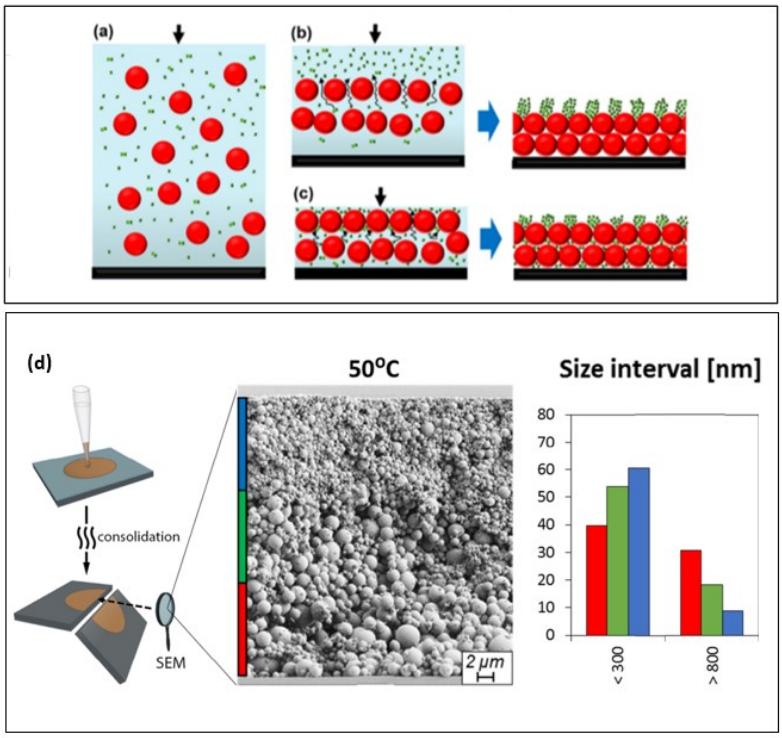

FIG. 7. Film formation model for drying blends of large latex (red) and small zinc oxide (green) particles: (a) initial configuration, homogeneous particle distribution, (b) slow evaporation scenario, and (c) fast evaporation scenario. Reproduced from ref. 53 with permission from the American Chemical Society (d) SEM cross sections, coating layer thickness, and number distribution by particle size for the bottom, middle, and top layers of the particulate assemblies. The histogram shows the numerical distribution by particle size for the bottom, middle, and top layers of particulate assemblies generated under optimized drying conditions. The initial volume fraction of LPs was the same in all situations (same number of particles). The particles were separated into two bins or fractions for ease of comparison and comparison. Namely, colloidal (<300 nm) and "settling" particles (>800 nm). The layer thickness (out-of-plane direction) was separated into three equidistant zones, bottom, middle, and top, each identified with a different color. Reproduced from ref. 54 with permission from the American Chemical Society.

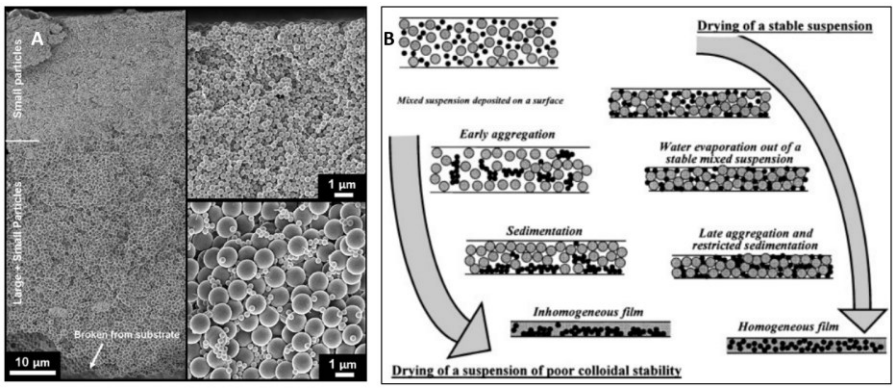

FIG. 8. (a) Cross-section image of a dried coating prepared from a bimodal aqueous silica dispersion. Top right: higher magnification image of top of coating. Bottom right: bottom of coating. Reproduced from ref. 59 with permission from the John Wiley & Sons Ltd. (b) the aggregation/sedimentation scenario leading to the final morphology of the dry film. Reproduced from ref. 60 with permission from the John Wiley & Sons Ltd.

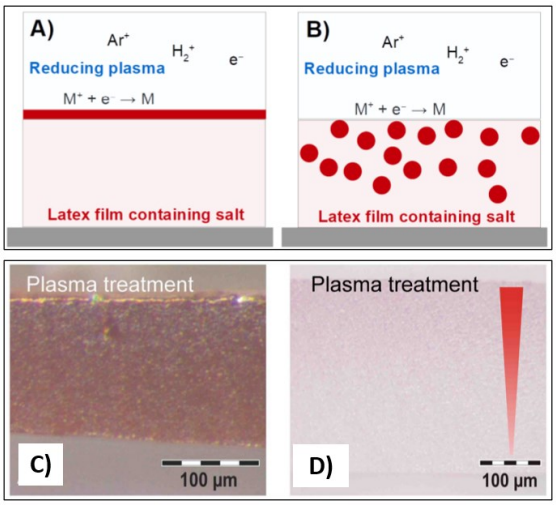

FIG. 9. Reductive processes at the top of the drying latex turn metal ions into bulk metal. (A) At high salt concentration, the metal forms a continuous layer on top of the latex film. (B) For moderate concentrations, particles are created inside the latex film. Micrographs showing cross sections. (C) A film with a metallic gold layer on the top. (D) A film showing a gradient in color. Gold particles are present throughout the entire film but are enriched at the top. Reproduced from ref. 61 with permission from the IOP Publishing.

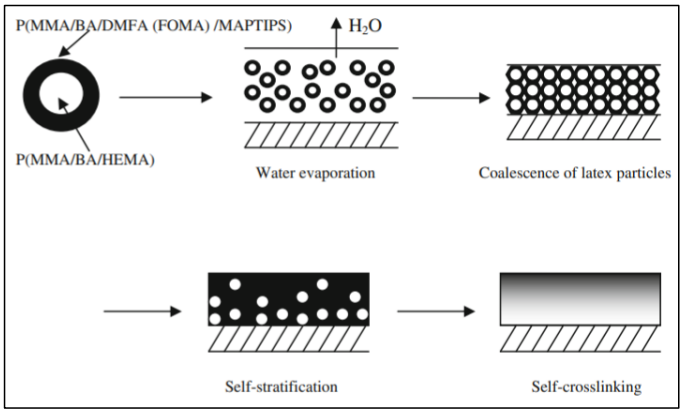

FIG. 10. Schematic representation of self-stratification process of the core-shell fluorine/ silicone-containing polyacrylate latex films. Reproduced from Ref. 68 with permission from the Springer Nature.

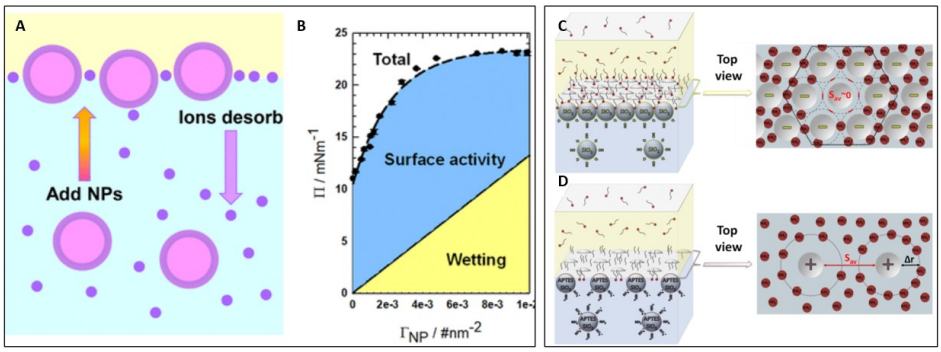

FIG. 11. (A) Schematic of single components (NP and $TPeA^+$ ion) adsorption at the toluene-water interface, Inset shows the legend for NP, ion-pair ligand, and $TPeA^+$ ion. Note here that the $TPeA^+$ ion is also part of the ion-pair covalently bound to the NP surface. (B) Total surface pressure caused by the adsorption of 5 nm NPs from pH 11.7 solutions. Adapted with permission from ref. 11. Copyright © 2018, American Chemical Society. Visual representation of the negatively (C) and positively (D) charged silica nanoparticles adsorbed at the decane-water interface and their interaction with the oil-soluble ODA surfactant molecules at intermediate to high concentrations. Adapted with permission from ref. 12. Copyright © 2018, American Chemical Society.

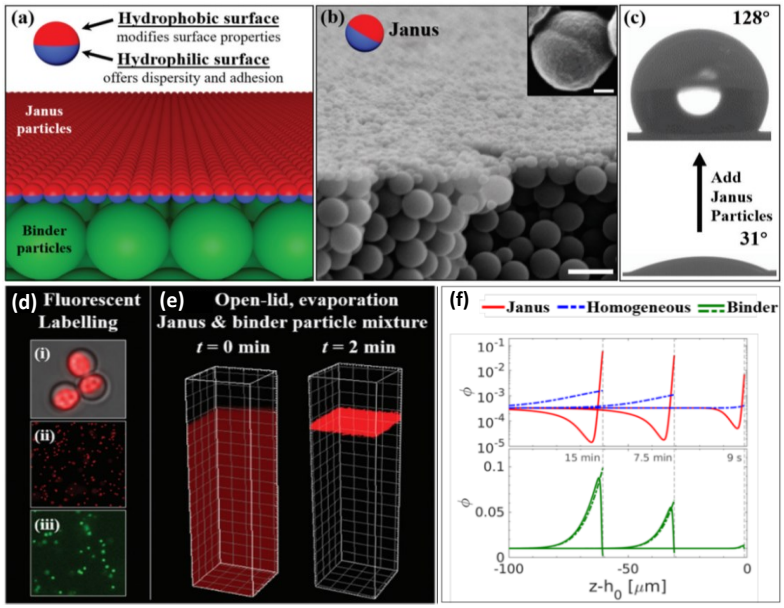

FIG. 12. (a) Schematic diagram for the coating structures formed by self-stratification of amphiphilic Janus particles mixed with binder particles; (b) SEM image of the cross-section view of dried coating structures. Scale bar is 2 μm. Inset shows the asymmetric morphology of a typical Janus particle with Janus balance (percentage of hydrophobic surface area) ~50%. Scale bar is 100 nm; (c) contact angles of the coating surface before and after adding the Janus particles; (d) fluorescent dye labelled Janus and binder particles: (i) hydrophobic side of 3 μm amphiphilic Janus particles labelled with Nile red; (ii) 400 nm amphiphilic Janus particles labelled with Nile red; (iii) homogeneous 1.3 μm binder particles labelled with green FITC; (e) particle dispersion composed of red amphiphilic Janus particles and unlabeled binder particles at different time points under the evaporation condition (open-lid); f) Theoretical comparison of time evolution of particle concentration profiles for the binary mixtures: Janus particles with binder particles (solid lines) and homogeneous particles with binder particles (dashed lines). Reproduced from ref. 31 with permission from the Royal Society of Chemistry.

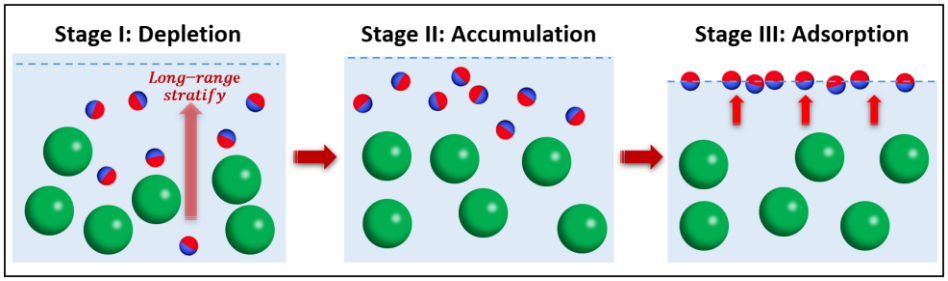

FIG. 13. Schematic representation of hypothetical model about Janus particle stratification: (Stage I) Depletion of binder particles from the interface due to the electrostatic repulsion; (Stage II) Accumulation of Janus particles to the interface due to osmotic pressure from binder particles; (Stage III) Adsorption of Janus particles at the interface due to their amphiphilicity and adsorption energy.